SUPERCONDUCTIVITY, INCLUDING HIGH-TEMPERATURE SUPERCONDUCTIVITY

Isolation of a Josephson qubit from the electromagnetic environment

V. I. Shnyrkov[a)]

B. Verkin Institute for Low Temperature Physics and Engineering of the National Academy of Sciences of Ukraine, 47 Lenin Ave., Kharkov 61103, Ukraine

A. M. Korolev

Institute of Radio Astronomy of the National Academy of Sciences of Ukraine, 4, Chervonopraporna st., Kharkov 61002, Ukraine

O. G. Turutanov[b)]

B. Verkin Institute for Low Temperature Physics and Engineering of the National Academy of Sciences of Ukraine, 47 Lenin Ave., Kharkov 61103, Ukraine

V. M. Shulga

Institute of Radio Astronomy of the National Academy of Sciences of Ukraine, 4, Chervonopraporna st., Kharkov 61002, Ukraine

V. Yu. Lyakhno

B. Verkin Institute for Low Temperature Physics and Engineering of the National Academy of Sciences of Ukraine, 47 Lenin Ave., Kharkov 61103, Ukraine

V. V. Serebrovsky

Southwest State University, 94, 50 years of October str., Kursk 305040, Russia
(Submitted June 3, 2015)
Fiz. Nizk. Temp. **41**, 1109–1118 (November 2015)

We consider two aspects of isolation of a Josephson flux (charge-flux) qubit from the external dissipative electromagnetic environment: (i) selecting an optimal topology of the superconducting qubit circuit and (ii) passive filtering of Planck radiation at the input of the qubit-state detection circuit. When reading the state of a macroscopic quantum object ("Schrödinger's cat") with the weak continuous measurement technique, the coupling to the environment, both direct and through the connected circuits, is the cause of the rapid loss of coherence of the superposition states. The coefficients of coupling to the external electromagnetic environment are discussed, as well as the problem of their minimization for flat (2D) and bulk (3D) designs of the qubit quantization loops. The analysis of the characteristics of low-temperature combined broadband filters designed to effectively reduce the electromagnetic noise in the control and measurement circuits is carried out. It is shown experimentally that a cryogenic Cu–CuO powder filter installed directly into the measuring circuit results in a significant suppression of the back action of a cooled HEMT amplifier to the qubit. [http://dx.doi.org/10.1063/1.4935839]

1. Introduction

One of the main physical problems in development of quantum circuitry that determines the fundamental possibility of building a workable quantum computer is achieving a sufficiently long lifetime of the coherent state of each qubit to allow completion of quantum computations and measurement of the final state of the qubit. The fundamental limit of the minimum decay time of the coherent state of a Josephson qubit τ_φ is determined by quantum fluctuations, resulting in radiative decay. The process of weak continuous quantum measurements,[1–4] associated with obtaining even a small information about the energy state of the qubit, is coupled with an increase in the decoherence rate according to Heisenberg's uncertainty principle. Coupling of the qubit with dissipative external control circuits (gates) through the external magnetic flux Φ_e and microwave fields results in additional decoherence, i.e., the loss of phase relations between the superposed components of the wave function.

Employing filters cooled down to mK temperatures in the measurement circuit[5,6] and weakening the coupling coefficients between the flux (charge-flux) qubit and the selective control circuits on the magnetic flux (charge) allows to reduce the effective temperature of the qubit to the refrigerator temperature of 10 mK (thermalize qubit).[7,8] In commonly used filters based on oxidized copper powder Cu-CuO,[5] high attenuation is attained in a wide frequency band due to the effective absorption of electromagnetic waves by normal-metal particles, which fill a section of a coaxial line. In some cases, the filter operation can be optimized by changing the intergrain capacitance and the resistivity of the grains by

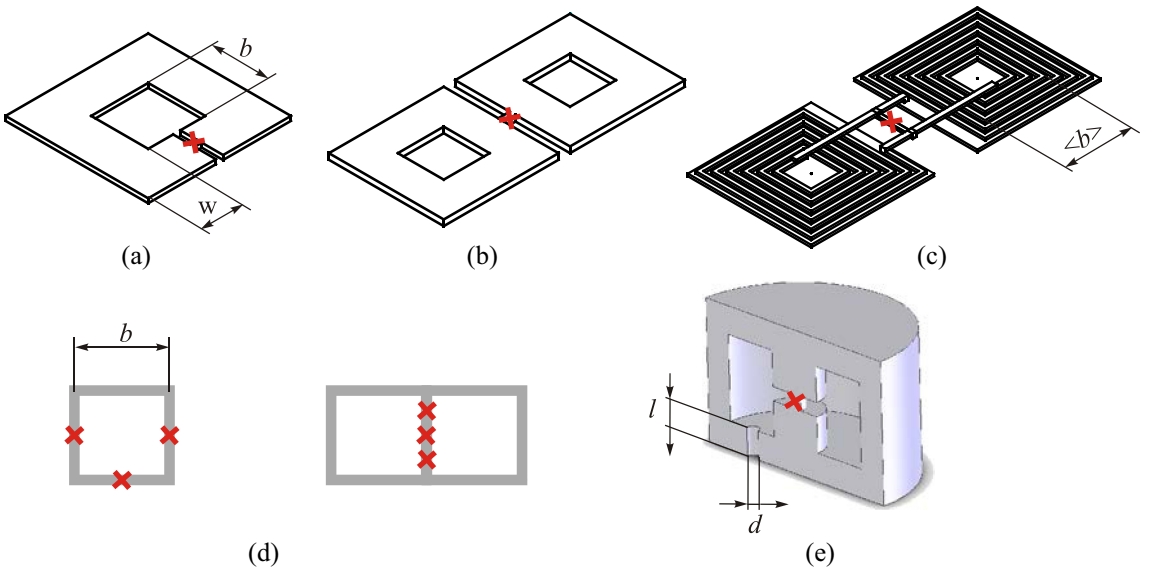

FIG. 1. Schematic topologies of the superconducting loops of flux qubits (crosses denote the Josephson junctions): dipole design with a large magnetic moment (pseudo qubit) (a); qubit with a quadrupole loop (b); quadrupole spiral loop, $\langle b\rangle \approx 10$ μm (c); three-junction qubits with a low magnetic moment, $b \sim 1$ μm (d); 3D toroidal qubit decoupled from the electromagnetic environment (e).

using powders of other materials (bronze, stainless steel).[9,10] Combined filters and chains of miniature cryogenic filters[5,6,10–13] based on thin-film meanders and wire spirals allow to achieve a total attenuation of -200 dB. The cutoff frequency of the filter is greatly reduced by adding lumped capacitance to such circuits (forming Pi-filters). Note that negligible dc losses in the dissipative filters based on a superconducting wire with a resistive shell allow currents up to 50 mA, when they are mounted in a dilution refrigerator with a temperature $T \approx 10$ mK.[9] In this study it was shown that for frequencies above 45 MHz, the noise spectrum of such a Pi-filter corresponds to equilibrium radiation with $T \approx 10$ mK. At frequencies below 45 MHz, the excessive noise can be effectively suppressed by filters with lumped parameters. In Ref. 14, filters designed to isolate pulse-control circuits have been considered. At $T = 4.2$ K, the filters showed 80 dB attenuation and wave impedance $Z_\omega \sim 50\,\Omega$ at 10 GHz. The absence of excess noise when using a stripe filter $Z_\omega \sim 50\,\Omega$ mounted directly on the dilution chamber of a refrigerator at $T = 25$ mK has been shown in Ref. 15. Recently, it has been proposed to use a three-section filter design for a large number of control lines.[16] This approach is interesting from the point of view of filtering the control gates when studying the dynamics of multiple qubits.

As shown by the above experimental results, flux qubits can be sufficiently well isolated from the control circuitry both for low-frequency and pulse signals. For example, since the rate of decoherence of a qubit τ_φ^{-1} due to the energy of thermal fluctuations k_BT in the control circuit for flux Φ_e with a resistance R is proportional to the square of mutual inductance M between them[7]

$$\tau_\varphi^{-1} \approx M^2\pi^3(R_Q/R)(E_J/\Phi_0^2)^2(k_BT/\hbar), \qquad (1)$$

the filter proposed in Ref. 9 allows to reduce it by almost two orders of magnitude by increasing the control current by an order of magnitude. Here $R_Q = h/e^2 \approx 25.8\,\text{k}\Omega$ is the quantum resistance, $h = 2\pi\hbar$ is the Planck constant, e is the electron charge, $\Phi_0 = h/2e \approx 2.07 \times 10^{-15}$ Wb is the magnetic flux quantum, and $E_J = I_c\Phi_0/2\pi$ is the Josephson energy of a junction with the critical current I_c. The rate of decoherence of a qubit coupled to a resonant circuit, which has been discussed in detail in Ref. 8, cannot be reduced in a similar way since M for this circuit is fixed by the condition of optimum matching the signal/noise ratio of the measuring channel. Coupling of a large number of superconducting qubits comprising the quantum computer circuitry with the electromagnetic environment can form a complex nonlinear system with additional decoherence effects. Therefore nowadays, in the process of development and design of "hardware," the search for optimal solutions for the measurement channel and the suppression of direct coupling of a superconducting flux qubit with the dissipative environment are important tasks of quantum-circuitry engineering.

In this paper we discuss the topology of a flux qubit and the passive filtering of the measurement channel to isolate the quantum system during the measurements.

2. Isolation of a superconducting flux qubit through its topology

A Josephson qubit is a quantum-coherent *macroscopic object*, the coupling of which to external electromagnetic fields via emission (absorption) of photons is determined by its size and topology. In the simplest case, a flux qubit (Fig. 1(a)) consists of a superconducting loop of size $b \times b$ with a geometric inductance L, closed by a single Josephson junction with a critical current I_c. The supercurrent in the loop is related to the phase difference of the order parameter at the Josephson junction through the equation $I_s = I_c \sin\varphi$, where $\varphi = 2\pi\Phi/\Phi_0$ is the phase difference at the contact and Φ is the magnetic flux through the loop. Thus, a flux qubit is formally described by the same Hamiltonian as an rf SQUID quantization loop:

$$H = \frac{(\Phi - \Phi_e)^2}{2L} - E_J\cos\varphi + \frac{q^2}{2C_J}. \qquad (2)$$

Here, Φ_e is the external magnetic flux applied to the qubit and q is the polarization charge on the Josephson junction

capacitance C_J. In a single-junction rf SQUID and flux qubit, the last term vanishes. The energy of a flux qubit, which is defined by the first two terms of Eq. (2), will have two degenerate states corresponding to two oppositely directed currents when the external flux $\Phi_e = \Phi_0/2$ and the following condition is satisfied:

$$\beta_L = L/L_J = 2\pi LI_c/\Phi_0 > 1. \quad (3)$$

For a tunnel junction with $I_c \approx 1$ μA, the above condition is satisfied (similar to the hysteresis mode of an rf SQUID) for a sufficiently large geometric inductance of the qubit $L \geq 3 \times 10^{-10}$ H.

Quantum coherent transitions between two degenerate states may occur when using a Josephson tunnel junction with a negligible quasiparticle current[17] and low capacitance C_J, which plays the role of mass in the quasi-classical equation of motion. For quality tunnel junctions Nb-AlO_x-Nb and Al-Al_2O_3-Al with $I_c \approx 1$ mA and resistance $R_T = \Delta(0)R_Q/(8E_J) \approx 4.7$ kΩ and 0.31 kΩ for niobium and aluminum junctions, respectively, the self-capacitance of the junction is in the range $C_J = 1$–10 fF.

When designing a qubit, the height of the "cosine" potential barrier $\Delta U \sim LI_c \sim \beta_L$ (2) is chosen so that the probability of an over-the-barrier transition due to the energy of thermal fluctuations, which is proportional to $\exp(-\Delta U/k_BT)$, is small, while the tunneling rate remains significant. Under these conditions, the degenerate energy levels of two classically uncoupled wells become split by $\delta E_{01} = E_1 - E_0$ (caused by the current oscillations due to coherent tunneling), forming a quantum superposition of two ground states in a symmetric potential

$$|\Psi\rangle = \alpha|0\rangle + \beta|1\rangle \quad (4)$$

with equal coefficients $\alpha = \beta = 2^{-1/2}$.

For not too deep wells ($1.5 > \beta_L > 1$), the current oscillation frequencies, taking into account the capacitance of the tunnel junction, can be $f = \delta E_{01}/h = 3$–10 GHz. Due to the high values of inductance required (Eq. (3)) and circulating currents I_S, the magnetic moment in a single-junction flux qubit reaches macroscopic values $\mu_S \approx 10^9$–10^{10} μ_B (a macroscopic quantum system with pseudospin 10^{-12}–10^{-13} J/T).[18] Here $\mu_B = 0.93 \times 10^{-23}$ J/T is the Bohr magneton. Compared to other solid-state qubits, such macroscopic magnetic moments are well-measurable. However, the cost to pay is strong interaction with the external electromagnetic environment and, as a consequence, an increase in the decoherence rate.

For a film (2D) qubit design with a linear contour dimension $b = S^{1/2}$ and inductance $L \approx 1.25\,\mu_0 b = 3 \times 10^{-10}$ H for $b \ll w$ (Fig. 1(a)), we obtain $b \sim 190$ μm. For the frequencies of state superposition $f \approx 10$ GHz, the qubit size is significantly smaller than the length of the electromagnetic wave in a vacuum, $b \ll \lambda = c/f$, and for the calculation of decoherence rate due to radiation (absorption) of energy, it can be considered as a point magnetic dipole. Analysis in this limit and numerical evaluation, carried out in Ref. 19, show that the rate of decoherence only due to the emission of photons is $\tau_\varphi^{-1} \sim 10^7$ s^{-1}. Taking into account an additional contribution to the decoherence rate due to the absorption of photons (see below) of the external electromagnetic field with extremes at $b/\lambda = 1, 1.5, 2, \ldots$ gives even greater value $\tau_\varphi^{-1} \geq 10^8$ s^{-1}. Therefore, the design shown in Fig. 1(a), is a pseudo qubit due to the radiation losses $\sim|\ddot{\mu}_S|^2$.

Isolation of flux and charge-flux qubits[20–22] with large magnetic moments μ_S can be improved by switching to the topology proposed by Zimmerman[23] for rf SQUIDs (Fig. 1(b)). In this loop geometry, almost identical currents flow in opposite directions, the total magnetic moment tends to zero, and the coupling between the qubit and external environment is limited to a weak magnetic quadrupole radiation (absorption). However, it should be noted that due to the asymmetric effect of the control and signal registration circuits, the magnetic moment of the qubit remains finite, usually $\delta\mu_S/\mu_S \sim 0.1$. Further reduction of the magnetic moment μ_S of a qubit with large inductance $L \sim n^2 \langle b \rangle$ can be achieved by adopting a spiral 2D topology (Fig. 1(c)), for which the characteristic size can be $\langle b \rangle \sim 10$ μm. However, even in this case it is necessary to take into account the reduction of design symmetry due to coupling with external circuits.

Dramatic reduction of the magnetic moment and high coefficients of qubit isolation from the external environment are automatically realized in a film (2D) qubit with three Josephson junctions, proposed in Ref. 24 (Fig. 1(d)). Linear size of the qubits with three Josephson junctions, their inductance and circulating current are sharply reduced: $b \approx 1$–5 μm, $L = 10^{-12}$–10^{-11} H, $\Phi \cong \Phi_e$,[25] so the decoherence due to radiation (absorption) of photons becomes insignificant. For example, for a three-junction qubit, a formal estimate of τ_φ^{-1} due to the coupling with dissipative environment shows[24] that for $b \approx 1$ mm, $f = \delta E_{01}/h \approx 10$ GHz and the circulating current of 1 nA, the decoherence rate $\tau_\varphi^{-1} \sim 10^{-7}$ s^{-1}. However, internal decoherence sources arising due to specific implementation of a micron-size flux qubit, the effect of control and signal detection circuits result in a substantial increase in the rate of relaxation and decoherence.[26] In addition, the use of flux qubits with inductance $L \approx 10^{-12}$ H in the quantum interface complicates the implementation of the concept of an ensemble of strongly coupled qubits.

The importance of optimization of a qubit and delicate design of the signal detection circuit has been shown in Refs. 27 and 28 for the Josephson junctions shunted with additional capacitance, which were loosely coupled to the electromagnetic field of high-Q bulk 3D resonators with natural frequencies $\hbar\omega_T \gg k_BT$. In an optimally isolated design, a total lifetime of the coherent superposition of $\tau_\varphi \approx 10^{-4}$ s has been found experimentally

$$\tau_\varphi^{-1} = \tau_{\varphi 0}^{-1} + (2\tau_1)^{-1}, \quad (5)$$

where $\tau_{\varphi 0}$ is the pure phase decoherence time and τ_1 is the energy relaxation time.

Fig. 1(e) shows schematics of a qubit with a toroidal 3D loop closed by a Josephson junction. In this arrangement, the superconducting loop of the qubit is virtually isolated from the external electromagnetic environment. Coupling of the qubits with the environment through the wires of the control circuits (TEM-mode) is suppressed by ladder-type filters. Radiation at the frequencies below the critical ($f_c \approx 1.75 \times 10^8/d$, waveguide modes) virtually does not reach the cavity with the qubit due to a large ratio of the length l to the diameter of the holes: $l/d \geq 8$ (Fig. 1(e)). In the actual

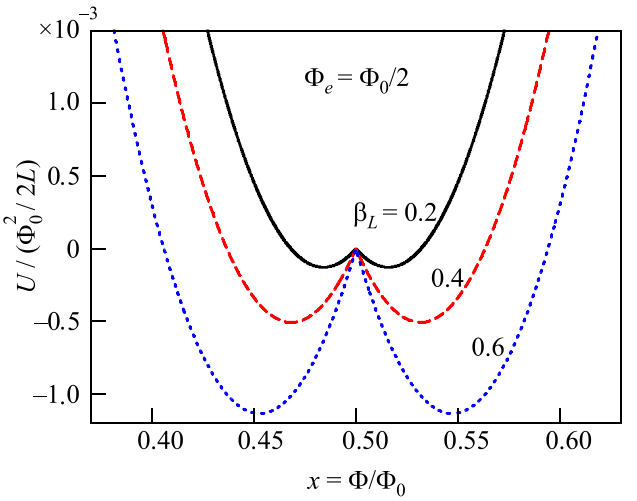

FIG. 2. Normalized potential energy of the superconducting loop with an ScS-contact as a function of the dimensionless magnetic flux in the loop for vanishing temperature.

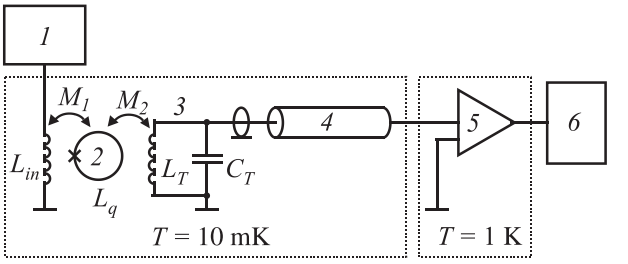

FIG. 3. Block diagram of the measuring path for weak continuous quantum measurements of the state of a flux qubit. 1—excitation generator, inductively coupled to the qubit L_q; 2—qubit; 3—L_TC_T tank circuit or resonator; 4—dissipative powder filter; 5—cooled amplifier; 6—electronic signal detection circuit located at room temperature. M_1 and M_2—mutual inductances.

circuit, the coupling of such qubit with other qubits and the measurement path is achieved by using a superconducting coaxial cable connected directly to the case and preventing the penetration of external electromagnetic fields through a hole in the case. The high-frequency part of the spectrum, from the millimeter waves to visible range, is effectively suppressed by cooled dissipating powder filters (Refs. 9–16, see details below).

Replacing the tunneling Josephson junction with a contact of ScS type, modifies condition (3) due to the unusual current-phase relation,[29,30] which in the limit of low temperatures has the form:

$$I_s = I_c \sin\frac{\varphi}{2}\,\mathrm{sgn}\,[\sin\varphi]. \tag{6}$$

Due to this unusual dependence, for a qubit with an ScS-type junction, a double-well potential can be obtained at lower critical currents (formally for $\beta_L < 1$)

$$U(\Phi,\Phi_e) = \frac{(\Phi-\Phi_e)^2}{2L} - E_J\left|\cos\frac{\varphi}{2}\right|, \quad E_J = \frac{I_c\Phi_0}{2\pi}. \tag{7}$$

This property of the potential (7) allows a significant increase in the tunneling rate and reduction of the magnetic moment μ_S of a flux qubit (and radiation intensity) by reducing the area of the barrier (quantum-mechanical action) and the magnitude of the circulating current. The set of the dependences of the potential energy $U(\Phi)$ of a superconducting loop closed by an ScS contact, for different values of the parameter β_L, which is proportional to the critical current I_c, is shown at the degeneracy point $\Phi_e = \Phi_0/2$ in Fig. 2. Calculations[31] show that, at a temperature of 10 mK (the temperature at which the following measurements on a charge-flux qubit with a dissipating powder filter were performed) the height of the potential barrier ΔU exceeds the energy of thermal fluctuations k_BT already starting from $\beta_L > 0.055$. For a qubit inductance $L_q = 785$ pH, it corresponds to the condition $I_c > 23$ nA, which is satisfied with a large margin. Note that smearing of the top of the barrier, calculated by the method described in Ref. 32, is negligible for the indicated parameters, which validate the use of Eqs. (6) and (7), which were derived, strictly speaking, at zero temperature.

Due to the high screening coefficient of the external electromagnetic fields, rf SQUIDs with toroidal quantization loops were used by us in the studies of sensitivity in the hysteresis-free $\beta_L < 1$ and hysteresis $\beta_L > 1$ regimes[33–35]

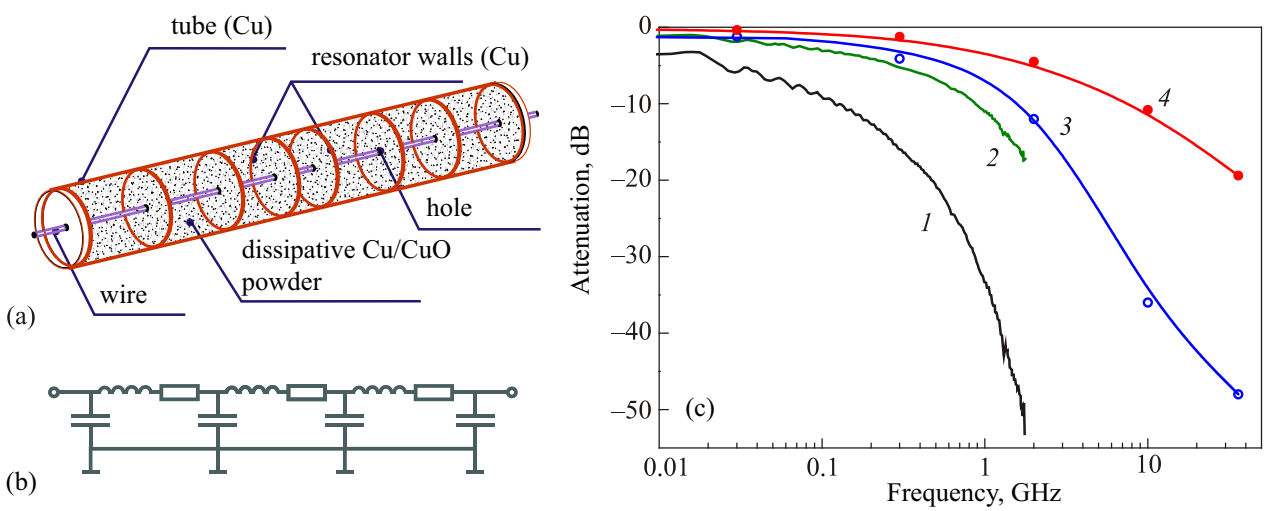

FIG. 4. Coaxial partitioned powder filter: design (a); simplified equivalent circuit (b); frequency dependences of the damping coefficients measured at $T = 290$ K (c): 1—coaxial cable AcAc20 of 3 m length, 2—the same cable of 1 m length, 3—coaxial partitioned powder filter of 10 cm length, 4—the same filter of 3 cm length.

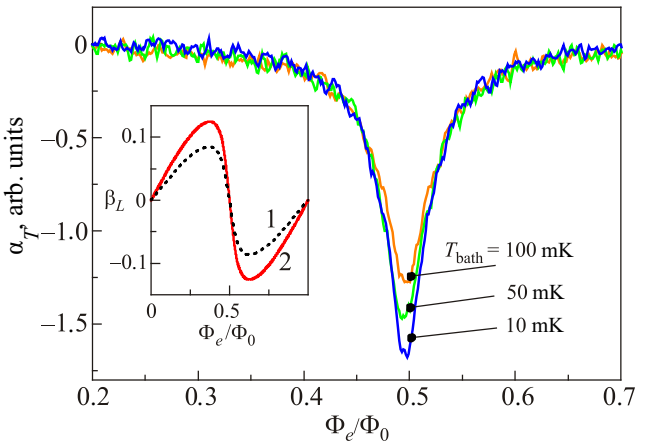

FIG. 5. Measurement of effective quantum inductance $L_{Q\text{eff}}$: dependence of the phase α_T of rf oscillations in the resonant circuit on the external magnetic flux for different temperatures of the dilution refrigerator with a partitioned powder filter; $\alpha_T \sim L^{-1}_{Q\text{eff}}$ for small α_T. The inset shows the dependence of the parameter $\beta_L(\Phi_e)$ on the external magnetic flux for a charge-flux qubit with the ratio of the critical currents of the junctions $I_{c2}/I_{c1} \approx 0.69$ at $T = 10$ mK: 1—without a filter, 2—with a powder filter installed at $T = 10$ mK.

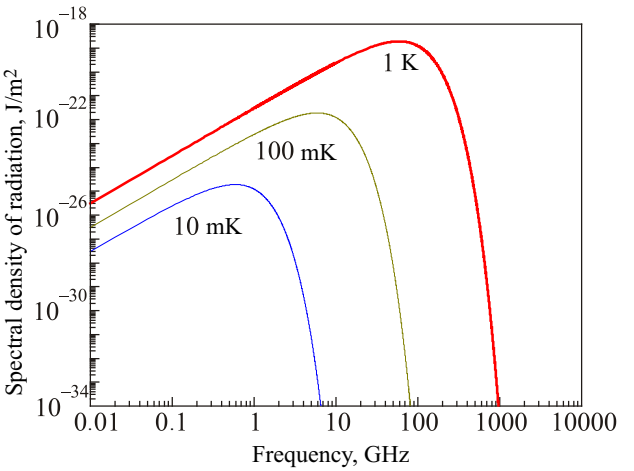

FIG. 6. Spectral density of the equilibrium radiation energy for three different values of the integral brightness temperature T^* of the signal detection and amplification path.

and in the study of the macroscopic (including the resonant) tunneling.[36]

Using a modified 3D toroidal loop (with a reduced geometrical capacity and the parameters $l_0 \approx 4 \times 10^{-3}$ m and $2r_0 \approx 5 \times 10^{-4}$ m) and pure ScS contact, we have obtained and analyzed signal and IV-characteristics of an rf SQUTRID (superconducting qutrit detector).[37,38] However, the experimental dependence of the local curvature of the ground superposition level of an rf SQUTRID on the external magnetic flux $\partial E_{0S}/\partial\Phi_e(\Phi_e)$ and IV-characteristics are in good agreement with theory only when a certain radiation excess of noise origin is taking into account,[38] which, as we suppose, is induced in the qubit by the cooled (first) stage of the amplifier in the measurement circuit.

3. Qubit isolation from the measurement circuit

The problem of measuring the final quantum state is one of the major problems in all versions of quantum computers. Fig. 3 shows a typical block diagram of the measurement circuit for weak continuous quantum measurements on a flux qubit (or charge-flux qubit), which includes a measurement channel with a matching resonant circuit and a cooled HEMT (high electron mobility transistor) amplifier stage.

Analysis of the temperature dependences of the Rabi oscillations in charge-flux qubits[22,39,40] with planar topology (Fig. 1(b)), obtained using this measurement schematics (Fig. 3) but without the powder filter, shows that in the refrigerator with an operating temperature $T \approx 10$ mK the back action of the measurement circuit results in an increase in the integral effective temperature to $T_{\text{eff}} \approx 75$–$80$ mK. To our knowledge, the minimum values of $T_{\text{eff}} \approx 55$ mK for qubits achieved in Ref. 41 are also significantly higher than the operating temperature of the refrigerator.

Assuming that in the circuit shown in Fig. 3, the main contribution to the increase of the effective temperature of the qubit T_{eff} is associated with the back action of the resonant circuit, part of which is located at a temperature above 10 mK, and a cooled HEMT amplifier (type ATF35143 AGILENT) with a power consumption of 100 μW per stage, we directly filtered the high-frequency part of the spectrum by inserting a powder filter into the measurement path at 10 mK. The design of the coaxial combined powder filter, a simplified equivalent circuit of the filter and its frequency response showing the signal attenuation at the frequency $f_0 \approx 30$ MHz not exceeding 1 dB are shown in Fig. 4. The filter consists of a copper tube of 3 cm length, filled with fine ($\sim$20–30 μm) oxidized copper powder. The inside of the filter is divided into sections by copper washers that have no contact with the central wire and form a structure of an LC-filter.

It is well known[42] that the path (filter) loss increases the equivalent noise temperature of the amplifier

$$T_{nf} = KT_n + (K-1)T_f \approx 1.26T_n, \tag{8}$$

where T_{nf} is the equivalent noise temperature of the cooled amplifier with a filter, K is the loss factor at the signal frequency, T_f is the physical temperature of the filter. To assess the efficacy of filtering the high-frequency part of the back-action spectrum, we measured the effective quantum inductance $L_{Q\text{eff}}$,[8,38] which depends on the local curvature of the ground energy level of a charge-flux qubit,[8,22] as a function of the external magnetic flux and magnetic flux fluctuations (effective temperature) for three different temperatures of the dilution refrigerator (see Fig. 5). It should be noted that for the weak continuous measurements of flux and charge-flux qubits controlled by a flux gate, the same scheme is used (Fig. 3), and the problem of isolation of a qubit from the electromagnetic environment can be solved in the same way. The inductance of the charge-flux qubit was $L_q = 785$ pH, the quality factor of the resonant circuit $Q = 685$, the natural frequency $f_0 = 27.39$ MHz, $k^2Q \approx 1$. As can be seen from this data, the coupling coefficient $k = M_2/(L_qL_T)^{1/2}$ between the qubit and the tank circuit is small, resulting in a weak effect of changes in non-linear inductance of the qubit on the rf frequency of circuit oscillations. According to Refs. 8, 22, and 38, a small reactive contribution of a qubit causes, respectively, a slight change in the measured phase α_T of rf oscillations in the resonant circuit, which in this linearized case is proportional to the inverse effective quantum inductance of the qubit as a function of the external magnetic flux $L^{-1}_{Qeff}(\Phi_e)$. Similar measurements have been carried out in Ref. 39 and theoretically validated in Ref. 43.

It is clearly seen that as the bath temperature is lowered from 100 to 50 mK and then further to 10 mK, the absolute value of the effective quantum inductance increases. In the experiments with no filter, the curvatures at $T = 50$ mK and 10 mK are practically the same. This means that despite a 30% increase in the measurement uncertainty associated with the attenuation increase in the signal path, the back action on the qubit can be reduced by optimal broadband filtering of high frequencies.

Isolation improvement of the charge-flux qubit from the measurement path containing a HEMT amplifier by direct filtration was confirmed by measuring the dependences $\beta_L = 2\pi L I_s(\Phi_e)/\Phi_0$ on the external magnetic flux at a constant refrigerator temperature $T = 10$ mK, shown in the inset to Fig. 5. Without a filter, the maximum value was $\beta_{L\max} \approx 0.085$ ($I_{c\max} \approx 35.65$ nA), while with a cooled powder filter the measured values increased to $\beta_{L\max} \approx 0.125$ ($I_{c\max} \approx 52.4$ nA).

One of the simplest ways to interpret the results, is by introducing an integral brightness temperature T^*, characterizing the radiation of the measuring path and its back action on the qubit. Directly at the HEMT input, there is a thermal mechanism for generating noise due to ohmic losses in the input circuits of the transistor. Integral radiation is characterized by: (i) a temperature close to the physical temperature of the crystal lattice of the HEMT transistor, which might be higher than the refrigerator temperature due to power dissipation in the active zone of the channel; (ii) radiation of the two-dimensional gas of "hot" electrons in the saturated zone of the HEMT channel,[44] which is transferred from the "output" to the "input" through the inner drain–gate capacitance of the transistor, as well as by exciting waveguide modes inside the transistor casing by the output circuit; (iii) radiation from the passive elements of the measuring path, located at $T >$ 10 mK. For the transistors of type ATF35143 (AGILENT), the characteristic value of the back action parameter in the S-matrix (S_{12}) is $-20\ldots -30$ dB at 1 GHz, and it increases with frequency following an almost linear relation. For an unmatched amplifier with high input impedance (the parameter S_{12} is specified for a 50 Ω tract), the back action increases somewhat. It is evident that, having a HEMT amplifier with a power consumption of about 100 μW in the temperature range $T = 1$–1.5 K, we obtain an integral brightness temperature $T^* \geq 1$ K and the frequency dependence of the intensity of equilibrium radiation $S(f, T^*) = hf/[\exp(hf/k_BT^*) - 1]$, which lies above the curve with $T^* = 1$ K in Fig. 6. In this case, a cooled powder filter with the attenuation of 6 dB/octave (above 500 MHz) partially isolates the qubit from the high-frequency component of the spectrum, while introducing losses of only ~1 dB at 30 MHz in the measurement path.

The isolation of a qubit from the measurement path can be improved by using the HEMT amplifier in the unsaturated mode.[45,46] These studies demonstrated the ability to reduce the power consumption in HEMT amplifiers down to 10^{-6} W per stage for the operating frequencies $f_0 \leq 1$ GHz and to less than 100 nW in the amplifiers for the range of $f_0 =$ 30–100 MHz. Because of the low power dissipation, HEMT amplifiers operating in the unsaturated mode can be placed at the refrigerator temperature $T \leq 50$ mK,[47] which automatically reduces the radiation of passive elements of the measurement path, reducing the brightness temperature T^* to 100–10 mK (Fig. 6).

4. Discussion

Superconducting quantum computer should consist of an ensemble of selectively controllable, strongly coupled with each other and isolated from the external electromagnetic environment qubits, which allow the final quantum state at the output to be measured. Recently created special cryogenic filters[10–16] allow to effectively thermalize the selective control circuits (gates) at $T \approx 10$ mK and isolate flux (charge-flux) qubits from the electromagnetic noise of these circuits. As was shown in Ref. 48, the use of the local curvature (quantum inductance) of the ground superposition energy level of a qutrit allows to create a controllable coupling element, including those with a large (~1 K) interaction energy.

Consideration of the topological features of the superconducting 2D flux qubits (Figs. 1(a)–1(c)) shows that most of them, except three-junction qubits,[24,25] are efficient transceiver antennas in the case $b \approx \lambda$, and cannot be adequately isolated from the external electromagnetic environment. Remarkable features of the electrodynamics of the toroidal 3D design of a quantization loop[49,50] allows to isolate almost completely the superconducting flux qubits with superposed states (Fig. 1(e)) from the external low-frequency and high-frequency electromagnetic fields. It should be noted that the qubit proposed by Mooij[24] (Fig. 1(d)), for which in Ref. 50 it has been proposed to use a toroidal topology, is already essentially decoupled from the electromagnetic environment due to the extremely low magnetic moment. The use of weak coupling based on mesoscopic ScS contacts in a toroidal flux qubit allows obtaining double-well potentials at low critical currents of the contact (Fig. 2) and thereby reducing the total magnetic moment μ_S. Thus, practical hardware design of small quantum registers based on flux qubits with toroidal 3D design of the quantization loop does not look very problematic.

Isolating a qubit from the measurement path is the most difficult task of experimental physics. The results obtained by direct filtration of the brightness temperature of the measurement path (Fig. 5) based on a HEMT amplifier can certainly be improved in subsequent experiments. For example, increasing the operating frequency up to $f_0 \approx 0.5$–1 GHz and the quality factor Q of the resonant circuit to $Q \approx 10^4$ reduces automatically the interaction between the qubit and measurement channel due to the weakening of the coupling coefficient to $k^2 \approx 10^{-4}$ (while maintaining the condition $k^2Q \approx 1$). Estimates show that the use of HEMT amplifiers with sub-μW dissipation at low temperatures should lead to a decrease in the integral brightness temperature T^* by at least an order of magnitude. Moreover, in the modified measurement circuit for weak continuous measurements, the variations of the magnetic flux of the qubit can be detected by SQUTRID[38]—an ideal parametric amplifier using quantum inductance, which further reduces the "parasitic" coupling with the active HEMT-based element.

5. Conclusion

Coupling of a large number of qubits that form the circuit of a quantum computer with the electromagnetic environment can form a complex nonlinear system with additional decoherence effects. Thus, one of the major

challenges on the way to creating superconducting quantum computers is to suppress coupling of each of the qubits with the environment while maintaining a strong controllable coupling between the qubits (see, e.g., Ref. 48).

According to the authors, the optimal scheme of weak continuous measurements on the superconducting state of a flux (charge-flux) qubit should include:

– A qubit with 3D toroidal topology of the quantization loop, decoupled from the electromagnetic environment;[36–38,50]
– A constriction-type Josephson junction (ScS) of an atomic size (quantum point contact) in the quantization loop, which provides a large splitting energy in the qubit, high speed (tunneling rate) and an increased decoherence time Ref. 38 and references therein;
– A superconducting entirely dissipation-free qutrit detector (SQUTRID),[38] not contributing to the qubit decoherence rate;
– A high-Q resonant system for matching with a high input impedance HEMT amplifier, which also reduces the coupling coefficient between the qubit and the measurement path;
– Broadband dissipating combined powder filters in the measurement circuit with low attenuation at the operating frequency, which effectively eliminate the effect of the brightness temperature of the amplifier input on the qubit decoherence rate at the cost of minor overall sensitivity reduction of the measurement path;
– A cooled to tens of mK unsaturated HEMT amplifier with ultra-low power consumption.[45,47]

The work was performed within the framework of the fundamental research program of NASU, Grant Nos. 0112U002640 and 0112U000035.

[a]Email: shnyrkov@ilt.kharkov.ua
[b]Email: turutanov@ilt.kharkov.ua

[1]A. N. Korotkov and D. V. Averin, Phys. Rev. B **64**, 165310 (2001).
[2]D. V. Averin, in *Exploring the Quantum/Classical Frontier: Recent Advances in Macroscopic Quantum Phenomena*, edited by J. R. Friedman and S. Han (N. Publishers, Hauppauge, NY, 2002), p. 441; e-print arXive:cond-mat/0004364.
[3]A. Yu. Smirnov, Phys. Rev. B **68**, 134514 (2003).
[4]R. Ruskov and A. N. Korotkov, Phys. Rev. B **67**, 241305(R) (2003).
[5]J. M. Martinis, M. H. Devoret, and J. Clarke, Phys. Rev. B **35**, 4682 (1987).
[6]D. Vion, P. F. Orfila, P. Joyez, D. Esteve, and M. H. Devoret, J. Appl. Phys. **77**, 2519 (1995).
[7]Yu. Makhlin, G. Schön, and A. Shnirman, Physica C **368**, 276 (2002); Rev. Mod. Phys. **73**, 357 (2001).
[8]A. B. Zorin, Zh. Eksp. Teor. Fiz. **125**, 1423 (2004) [JETP **98**, 1250 (2004)].
[9]F. P. Milliken, J. R. Rozen, G. A. Kneefe, and R. H. Koch, Rev. Sci. Instrum. **78**, 024701 (2007).
[10]A. Fukushima, A. Sato, A. Iwasa, Y. Nakamura, T. Komatsuzaki, and Y. Sakamoto, IEEE Trans. Instrum. Meas. **46**, 289 (1997).
[11]H. le Sueur and P. Joyez, Rev. Sci. Instrum. **77**, 115102 (2006).
[12]A. Lukashenko and A. V. Ustinov, Rev. Sci. Instrum. **79**, 014701 (2008).
[13]K. Bladh, D. Gunnarsson, E. Hürfeld, S. Devi, C. Kristoffersson, B. Smålander, S. Pehrson, T. Claeson, P. Delsing, and M. Taslakov, Rev. Sci. Instrum. **74**, 1323 (2003).
[14]H. Bluhm and K. A. Moler, Rev. Sci. Instrum. **79**, 014703 (2008).
[15]D. H. Slichter, O. Naaman, and I. Siddiqi, Appl. Phys. Lett. **94**, 192508 (2009).
[16]S. Mandal, T. Bautze, R. Blinder, T. Meunier, L. Saminadayar, and C. Bäuerle, Rev. Sci. Instrum. **82**, 024704 (2011).
[17]A. J. Leggett, in *Chance and Matter: Les Houches Session XLVI*, edited by J. Souletie, J. Vannimenus, and R. Stora (Elsevier, Amsterdam, 1987), p. 395.
[18]J. R. Friedman, V. Patel, W. Chen, S. K. Tolpygo, and J. E. Lukens, Nature **406**, 43 (2000).
[19]E. M. Chudnovsky and A. B. Kuklov, Phys. Rev. B **67**, 064515 (2003).
[20]R. Whiteman, T. D. Clark, R. J. Prance, H. Prance, V. Schöllmann, J. F. Ralph, M. Everitt, and J. Diggins, J. Mod. Opt. **45**, 1175 (1998).
[21]D. Born, V. I. Shnyrkov, W. Krech, Th. Wagner, E. Il'ichev, M. Grajcar, U. Hübner, and H.-G. Meyer, Phys. Rev. B **70**, 180501(R) (2004).
[22]V. I. Shnyrkov, Th. Wagner, D. Born, S. N. Shevchenko, W. Krech, A. N. Omelyanchouk, E. Il'ichev, and H.-G. Meyer, Phys. Rev. B **73**, 024506 (2006).
[23]J. E. Zimmerman, J. Appl. Phys. **42**, 4483 (1971).
[24]J. E. Mooij, T. P. Orlando, L. Levitov, L. Tian, C. H. van der Wal, and S. Lloyd, Science **285**, 1036 (1999).
[25]I. Chiorescu, Y. Nakamura, C. J. P. M. Harmans, and J. E. Mooij, Science **299**, 1869 (2003).
[26]G. Burkard, D. P. DiVincenzo, P. Bertet, I. Chiorescu, and J. E. Mooij, Phys. Rev. B **71**, 134504 (2005).
[27]H. Paik, D. I. Schuster, L. S. Bishop, G. Kirchmair, G. Catelani, A. P. Sears, B. R. Johnson, M. J. Reagor, L. Frunzio, L. I. Glazman, S. M. Girvin, M. H. Devoret, and R. J. Schoelkopf, Phys. Rev. Lett. **107**, 240501 (2011).
[28]C. Rigetti, S. Poletto, J. M. Gambetta, B. L. T. Plourde, J. M. Chow, A. D. Corcoles, J. A. Smolin, S. T. Merkel, J. R. Rozen, G. A. Keefe, M. B. Rothwell, M. B. Ketchen, and M. Steffen, Phys. Rev. B **86**, 100506(R) (2012).
[29]I. O. Kulik and A. N. Omel'yanchuk, Fiz. Nizk. Temp. **3**, 945 (1977) [Sov. J. Low Temp. Phys. **3**, 459 (1977)].
[30]C. W. J. Beenakker and H. van Houten, Phys. Rev. Lett. **66**, 3056 (1991).
[31]O. G. Turutanov, V. A. Golovanevskiy, V. Yu. Lyakhno, and V. I. Shnyrkov, Physica A **396**, 1 (2014).
[32]O. G. Turutanov, V. Yu. Lyakhno, and V. I. Shnyrkov, e-print arXiv:1506.00953.
[33]V. I. Shnyrkov, V. A. Khlus, and G. M. Tsoi, J. Low Temp. Phys. **39**, 477 (1980).
[34]I. M. Dmitrenko, G. M. Tsoi, V. I. Shnyrkov, and V. V. Kartsovnik, J. Low Temp. Phys. **49**, 417 (1982).
[35]V. I. Shnyrkov and G. M. Tsoi, in *Principles and Applications of Superconducting Quantum Interference Devices*, edited by A. Barone (World Scientific Publishing, Singapore-London, 1992), p. 77.
[36]I. M. Dmitrenko, V. A. Khlus, G. M. Tsoi, and V. I. Shnyrkov, Fiz. Nizk. Temp. **11**, 146 (1985) [Low Temp. Phys. **11**, 77 (1985)].
[37]V. I. Shnyrkov, G. M. Tsoi, D. A. Konotop, and I. M. Dmitrenko, in *Single-Electron Tunneling and Mesoscopic Devices (SQUID'91)*, edited by H. Koch and H. Lübbig (Springer-Verlag, Berlin, 1991), p. 208.
[38]V. I. Shnyrkov, A. A. Soroka, and O. G. Turutanov, Phys. Rev. B **85**, 224512 (2012).
[39]M. Grajcar, A. Izmalkov, E. Il'ichev, Th. Wagner, N. Oukhanski, U. Hubner, T. May, I. Zhilyaev, H. E. Hoenig, Ya. S. Greenberg, V. I. Shnyrkov, D. Born, W. Krech, H.-G. Meyer, A. M. van den Brink, and M. H. S. Amin, Phys. Rev. B **69**, 060501 (2004).
[40]V. I. Shnyrkov, W. Krech, D. Born, V. V. Serebrovsky, and O. G. Turutanov, Fiz. Nizk. Temp. **40**, 1331 (2014) [Low Temp. Phys. **40**, 1035 (2014)].
[41]L. S. Bishop, J. M. Chow, J. Koch, A. A. Houck, M. H. Devoret, E. Thuneberg, S. M. Girvin, and R. J. Schoelkopf, Nat. Phys. **5**, 105 (2009).
[42]A. van der Ziel, *Noise. Sources, Characterization, Measurement* (Prentice-Hall, Englewood Cliffs, NJ, 1970).
[43]S. N. Shevchenko, Eur. Phys. J. B **61**, 187 (2008).
[44]A. M. Korolev, V. M. Shulga, O. G. Turutanov, and V. I. Shnyrkov, e-print arXiv:1502.06973.
[45]A. M. Korolev, V. I. Shnyrkov, and V. M. Shulga, Rev. Sci. Instrum. **82**, 016101 (2011).
[46]A. M. Korolev, V. M. Shulga, and S. I. Tarapov, Cryogenics **60**, 76 (2014).
[47]A. M. Korolev, V. M. Shulga, I. A. Gritsenko, and G. A. Sheshin, Cryogenics **67**, 31 (2015).
[48]A. A. Soroka and V. I. Shnyrkov, J. Low Temp. Phys. **172**, 212 (2013).
[49]G. N. Afanasiev and V. M. Dubovik, Fiz. Elem. Chastits At. Yadra **29**, 890 (1998) [Phys. Part. Nuclei **29**, 366 (1998)].
[50]A. M. Zagoskin, A. Chipouline, E. Il'ichev, J. R. Johansson, and F. Nori, e-print arXiv:1406.7678v1.

Translated by L. Gardt